

Adaptive Dictionary Sparse Signal Recovery Using Binary Measurements

Hossein Beheshti, Farzan Haddadi

Abstract—One-bit compressive sensing is an extended version of compressed sensing in which the sparse signal of interest can be recovered from extremely quantized measurements. Namely, only the sign of each measurement is available to us. There exist many practical applications in which the underlying signal is not sparse directly, but it can be represented in a redundant dictionary. Apart from that, one can refine the sampling procedure by using profitable information lying in previous samples. This information can be employed to reduce the required number of measurements for exact recovery by adaptive sampling schemes. In this work, we proposed an adaptive algorithm that exploits the available information in previous samples. The proof uses the recent geometric concepts in high dimensional estimation. We show through rigorous and numerical analysis that our algorithm considerably outperforms non-adaptive approaches. Further, it reaches the optimal error rate from quantized measurements.

Index Terms—One-bit, Dictionary sparse, Adaptive measurement, High dimensional estimation.

I. INTRODUCTION

IN classic signal acquisition theory, the first sufficient (although not necessary) condition is known as the Nyquist rate. But, through last decade, compressed sensing ignores this assumption and introduces new sampling schemes for some interesting classes of signals. In compressed sensing, samples are taken by linear measurements of the form

$$y_i = \langle \mathbf{a}_i, \mathbf{x} \rangle, \quad i = 1, \dots, m \quad (1)$$

where $\mathbf{a}_i \in \mathbb{R}^N$ are known measurement vectors, with elements drawn from a normal distribution and $\mathbf{x} \in \mathbb{R}^N$ is an unknown s -sparse signal which means \mathbf{x} has at most s nonzero entries and satisfies,

$$\|\mathbf{x}\|_0 := |\text{supp}(\mathbf{x})| = s. \quad (2)$$

With this assumption, if we take $m \sim s \log(N/s)$ measurements, typical compressed sensing results guarantee accurate recovery of the s -sparse signal, by solving the convex program (l_1 -minimization)

$$\min_{\hat{\mathbf{x}} \in \mathbb{R}^N} \|\hat{\mathbf{x}}\|_1 \quad \text{s.t.} \quad \mathbf{y} = \mathbf{A}\mathbf{x}, \quad (3)$$

with high probability (see [1], [2]).

In the compressed sensing theory, it is assumed that the measurements are exact. However, in practice, these measurements must be mapped into a finite symbol alphabet. Certainly, by using more accurate quantizers, the gap between practice and theory reduces, but it is an interesting question that what is the result of taking the reverse direction? This problem was investigated in [3]. According to [3], if we utilize the least resolution possible (just one bit), reconstruction of the signal still will be feasible.

The basic idea for employing binary measurement comes from one-bit analog to digital converters (ADC). In the ADC, sampling rate exponentially decreased by growing the number of bits. Therefore, if we exploit a single bit ADC—which implemented as a simple comparator—power utilization reduced and sampling rate can rise expeditiously. However, in some ultra-wideband digital receivers or massive multiple-input multiple-output (MIMO) systems, due to bandwidth, power or operational costs limitations, one-bit ADC is the only selectable option. Moreover, binary measurements, used in other applications such as binary regression, broadcasting, statistical modeling and etc (for more detail see [4], [5], [6], [7]).

Quantization is an irreversible process. Moreover, in one-bit compressed sensing, samples are taken from

$$\mathbf{y} = \text{sign}(\mathbf{A}\mathbf{x}). \quad (4)$$

consequently, \mathbf{y} contains no information about the magnitude and in this setup, we hope to discover the direction of vector \mathbf{x} . Fortunately, if we change comparison threshold from zero to a random variable for each measurement (for example, $\tau_i \sim N(0, 1)$), amplitude information is preserved. By this assumption, equation (4) changes to

$$\mathbf{y} = \text{sign}(\mathbf{A}\mathbf{x} - \boldsymbol{\tau}). \quad (5)$$

In the next sections, the difference between equation (4) and (5) is described from a geometric point of view.

The great part of research in the compressed sensing investigates reconstruction of the sparse signals. Nevertheless, there is a set of signals which become sparse after some transformations; for example, sinusoidal signals are sparse after Fourier transformation or images are sparse in the wavelet domain. If we use an orthogonal dictionary, compressed sensing results extend easily to this case. On the other hand, a set of signals—called dictionary-sparse signals—transfigured sparse in a nonorthogonal dictionary; for example, radar signals are sparse in Gabor frame. In [8], the problem of the redundant dictionary was solved and then, extended to the binary measurement [9].

A. Prior Work

In this section, we provide a concise survey of one-bit compressed sensing literature. In conventional CS, binary measurements are assumed to be scalar numbers; but [3] changed the sampling model and considered measurement as the sign of signal and developed a reconstruction algorithm by using this interpretation. In [10] the number of bits affecting was studied in high and low SNR. The result of [10] offers to use fewer bits in many practical applications. In the meanwhile, Several

new algorithms have been proposed; for example, matching sign pursuit (MSP), restricted-step shrinkage (RSS) and binary iterative hard thresholding (BIHT) (see [11], [12], [6]).

In [6], introduced a lower bound on reconstruction error as a function of sparsity level and the number of measurements. In addition, it proposed BeSE property of the measurement mapping which is analogous to RIP in conventional CS. In the following, [13], investigated the problem of one-bit CS from geometric view and used functional geometric analysis tools to provide an almost optimal solution to the problem of one-bit CS and in [14], noisy measurements were explored.

The work of [15] presented two algorithms for consummate (direction and norm) reconstruction with uniform guarantees. The first approach takes advantage of the random thresholds and the other method, separately predicts the direction and magnitude. The authors in [16] introduced an adaptive thresholding scheme which utilizes a generalized approximate message passing algorithm (GAMP) for recovery and thresholds update throughout sampling. Nevertheless, several explorations with different techniques accomplished to reduced reconstruction error. In [17], authors examined the one-bit Sigma-Delta quantization and achieved exponential accuracy in the oversampling ratio. The work [7] proposed an adaptive quantization and recovery scenario which attain an exponential decay of error in one-bit CS frameworks.

Recently works of Baraniuk et al. showed, both direction and magnitude of a dictionary-sparse signal can be recovered by a convex program or thresholding algorithm with strong guarantees [9]. To the best of our knowledge, this paper is the first article study adaptive dictionary-sparse algorithms in the context of one-bit compressed sensing.

B. Contributions

In this paper, we introduce an adaptive thresholding algorithm in the context of one-bit compressive sensing of dictionary-sparse signals. The system model is general and algorithm uses convex programming; therefore results can be used in any application.

Another key point is using an adaptive high-dimensional threshold to extract most information from each sample, which substantially improves performance and reduce reconstruction error. we also use geometric tool for building a qualitative understanding of algorithms procedure and shed light on proof steps.

There is nice intuition on algorithms procedure using *Hemisphere projection* (introduced in 3) which makes the algorithm comprehensible.

C. Outline

The paper is organized as follows: in Section II, first, we provide a short description of geometric tools that used throughout the paper. Then, we study some basic concepts in dictionary sparsity. In Section III, our system model with some dedicated definition has been explained. In Section IV, we present our algorithm for the recovery of the dictionary-sparse signal from binary measurements. In Section V, we investigate the performance of our work and compare it with

existing algorithms. Finally, in Appendix ??, we provide the proof of our main result.

D. Notation

Here we introduce the notation used throughout the paper. Vectors and matrix are denoted with boldface lowercase and capital letter respectively. \mathbf{v}^T and \mathbf{v}^* stand for transposition and hermitian of \mathbf{v} , respectively. Through the paper, C, c denote positive absolute constants which can be different from line to line. we use $\|\mathbf{v}\|_2 = \sqrt{\sum_i v_i^2}$ for the l_2 -norm of vector \mathbf{v} in \mathbb{R}^n , $\|\mathbf{v}\|_1 = \sum_i |v_i|$ for the l_1 -norm and $\|\mathbf{v}\|_\infty = \max_i |v_i|$ for the l_∞ -norm. $\|\mathbf{v}\|_0$ indicating number of non-zero elements of vector and if $\|\mathbf{v}\|_0 \leq s$ the vector \mathbf{v} called s -sparse. We also write $B_1^n := \{\mathbf{v} \in \mathbb{R}^n : \|\mathbf{v}\|_1 \leq 1\}$ for l_1 -ball, $B_2^n := \{\mathbf{v} \in \mathbb{R}^n : \|\mathbf{v}\|_2 \leq 1\}$ for l_2 -ball and $S^{n-1} := \{\mathbf{v} \in \mathbb{R}^n : \|\mathbf{v}\|_2 = 1\}$ for unit Euclidean sphere in \mathbb{R}^n .

Through the paper, $d_G(\mathbf{v}, \mathbf{u}) := 1/\pi \arccos\langle \mathbf{v}, \mathbf{u} \rangle$ denote the normalized geodesic distance between \mathbf{u} and \mathbf{v} on S^{n-1} and normalized Hamming distance between $\mathbf{a}, \mathbf{b} \in \{1, -1\}^m$ define as $d_H(\mathbf{a}, \mathbf{b}) := 1/m \langle \mathbf{a}, \mathbf{b} \rangle$.

II. PRELIMINARIES

Since the geometric intuition plays an important role in this article, we provide a short description of *Gaussian Width* and *Random Hyperplane Tessellation (RHT)*. Then, we review the basic concept of dictionary-sparse signals in the CS articles.

A. Gaussian Width

Generally, in the one-bit CS literature, the signal of interest is limited in some convex set according to the constraints of the problem. Convex bodies $\mathcal{K} \in \mathbb{R}^n$ are closed, bounded, convex sets with non-empty interior. The mathematical rules of convex bodies are studied under the title of *asymptotic convex geometry* and *geometric functional analysis*. As expressed in [18], in hyperbolic plans of a high dimensional convex body, \mathcal{K} consist a bulk and some outliers. If \mathcal{K} assumed to be an isotropic convex body, the volume distribution concentrated nearby the bulk (for more detail, see [18] Theorem 3.2).

Nevertheless, we need geometric tools to measure the size of the bulk. *mean width* compute the basic characteristics of \mathcal{K} . In the following, first, we discuss *spherical mean width* and *Gaussian mean width* then show the relation between them.

Let \mathcal{K} be a closed set in \mathbb{R}^n . The width of \mathcal{K} in the direction of $\hat{\mathbf{n}}$ is equal to the minimum distance of two parallel hyperplanes with normals $\hat{\mathbf{n}}$ that include \mathcal{K} . The width of \mathcal{K} defined as:

$$\sup_{\mathbf{u}, \mathbf{v} \in \mathcal{K}} \langle \hat{\mathbf{n}}, \mathbf{u} - \mathbf{v} \rangle$$

For example, as seen in Figs. 1, the width of \mathcal{K} in the direction of $\hat{\mathbf{n}}$ is equal to d .

Considering the direction vector $\hat{\mathbf{n}}$ uniformly distributed on S^{n-1} and compute the expectation, we can define the *spherical mean width* of \mathcal{K} :

$$\tilde{w}(\mathcal{K}) := \mathbb{E} \sup_{\mathbf{u}, \mathbf{v} \in \mathcal{K}} \langle \hat{\mathbf{n}}, \mathbf{u} - \mathbf{v} \rangle$$

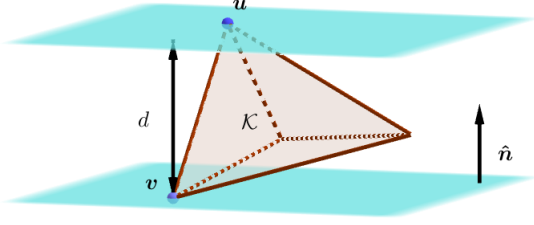


Fig. 1. Width of \mathcal{K} in the direction of \hat{n}

In practice, it is more convenient to acquire the bulk size from some direction with random and independent coordinates while the spherical mean width does not. For this reason, in practical terms, we use Gaussian mean width.

Definition 1 (Gaussian mean width). Let $\mathbf{g} \sim N(0, I_n)$ be a standard Gaussian random vector in \mathbb{R}^n . The Gaussian mean width of a bounded subset \mathcal{K} of \mathbb{R}^n is defined as

$$w(\mathcal{K}) := \mathbb{E} \sup_{\mathbf{u}, \mathbf{v} \in \mathcal{K}} \langle \mathbf{g}, \mathbf{u} - \mathbf{v} \rangle \quad (6)$$

For simplicity, we call Gaussian mean width as the *mean width* in the rest of this paper. By considering $\hat{\mathbf{n}} = \mathbf{g} / \|\mathbf{g}\|_2$, we can write spherical mean width as

$$\tilde{w}(\mathcal{K}) := \mathbb{E} \sup_{\mathbf{u}, \mathbf{v} \in \mathcal{K}} \langle \mathbf{g} / \|\mathbf{g}\|_2, \mathbf{u} - \mathbf{v} \rangle$$

since the direction and magnitude of a standard Gaussian random vector are independent, the relationship between spherical mean width and the mean width is

$$w(\mathcal{K}) = \mathbb{E} \|\mathbf{g}\|_2 \tilde{w}(\mathcal{K}).$$

In the following, we use the mean width to compute the size of the feasible set and limit the error.

B. Random Hyperplane Tessellation

As stated above, by using the measurement model (4) magnitude information was eliminated. In this case, the signal of interest \mathbf{v} considered to be normalized ($\|\mathbf{v}\|_2 = 1$) or equivalently the signal \mathbf{v} chosen from S^{n-1} and \mathbf{a}_i denote normal vector of hyperplanes which pass through the center of sphere. The measurements vector coordinates (y_i) specified which side of the hyperplane is valid. The geometric interpretation of problem in \mathbb{R}^3 is shown in Fig. 2.

It is obvious that if we take more measurements, the number of hyperplanes goes across the set \mathcal{K} increased, and reconstruction error decreased. The work of [19], shown the number of hyperplanes is depended on the mean width of the set \mathcal{K} with a constant multiplicative factor. Before expressing the main result of [19], it is necessary to define the δ -uniform tessellation which is stated in the following.

Definition 2 (δ -uniform tessellation). [19, Definition 1.1] Let \mathcal{K} be a subset of S^{n-1} . Consider m hyperplanes in \mathbb{R}^n and let $d(\mathbf{u}, \mathbf{v})$ denote the fraction of hyperplanes that separate points $\mathbf{u}, \mathbf{v} \in \mathcal{K}$. We say the set \mathcal{K} has been δ -uniform tessellated if

$$|d(\mathbf{v}, \mathbf{u}) - d_G(\mathbf{v}, \mathbf{u})| \leq \delta,$$

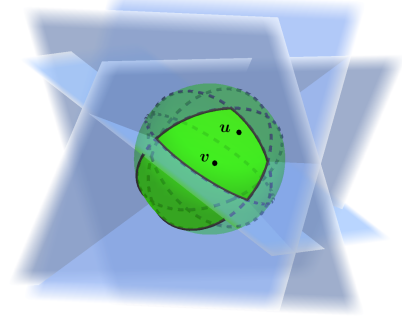


Fig. 2. The geometric interpretation of hyperplane tessellation

for given $\delta > 0$.

In our application, if we suppose rows of \mathbf{A} as the hyperplanes normal vectors and use measurement model (4), $d(\mathbf{u}, \mathbf{v})$ is identical to normalized Hamming distance ($d_H(\mathbf{z}, \mathbf{t})$) between $\mathbf{z} := \text{sign}(\mathbf{A}\mathbf{u})$ and $\mathbf{t} := \text{sign}(\mathbf{A}\mathbf{v})$. The next theorem bound the number of measurements (or equivalently hyperplanes), by using the mean width of \mathcal{K} .

Theorem 1 (Random uniform tessellation). [19, Theorem 1.2] Consider a subset $\mathcal{K} \subset S^{n-1}$ and let $\delta > 0$. Let

$$m \geq C\delta^{-6}w(\mathcal{K})^2$$

and consider an arrangement of m independent random hyperplanes in \mathbb{R}^n uniformly distributed according to the Haar measure. Then with probability at least $1 - 2\exp(-c\delta^2 m)$, these hyperplanes provide a δ -uniform tessellation of \mathcal{K} .

In the sampling model (4), the Theorem 1 result relates the number of measurements to the squared mean width of the set \mathcal{K} . For example, let \mathbf{u} and \mathbf{v} be two points on the S^{n-1} and coordinates of hyperplanes normal vectors draw from standard normal distribution and some fixed $\delta > 0$. If we take $m \geq C\delta^{-6}w(\mathcal{K})^2$ measurements and the hypothesized points satisfied Definition 2 condition, then, \mathbf{u} and \mathbf{v} are in the same cell with high probability (see Fig. 2).

We use the Theorem 1 extension to bound reconstruction error as a function of m .

C. Dictionary Sparsity

As mentioned above, in many practical applications the signal of interest is not sparse directly or respect to an orthogonal basis. In this section, we investigate the nonorthogonal dictionary. We denote the sparse signal by $\mathbf{x} \in \mathbb{R}^N$ and $\mathbf{D} \in \mathbb{R}^{n \times N}$ stand for the redundant dictionary ($N \gg n$) and our signal $\mathbf{f} \in \mathbb{R}^n$ is expressed as $\mathbf{f} = \mathbf{D}\mathbf{x}$. The coherence $\mu = \mu(\mathbf{D})$ of the matrix \mathbf{D} is defined as

$$\mu := \max_{1 \leq i \neq j \leq N} \frac{|\langle d_i, d_j \rangle|}{\|d_i\|_2 \|d_j\|_2},$$

where d_i and d_j denote columns of \mathbf{D} . The dictionary \mathbf{D} called *incoherent* for a small value of μ . In this situation, the product $\mathbf{A}\mathbf{D}$ is still Gaussian and standard compressed sensing guarantees accurate recovery from $\mathbf{y} = \mathbf{A}\mathbf{f} = \mathbf{A}\mathbf{D}\mathbf{x}$.

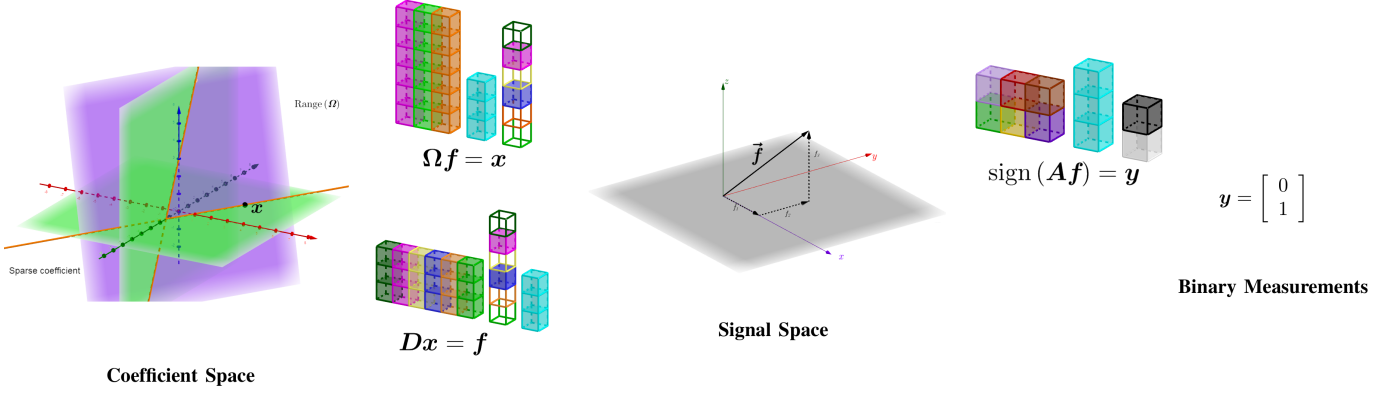


Fig. 3. The process of constructing a dictionary sparse signal and taking measurements in the binary forms.

Nevertheless, redundant dictionaries are of our considerable interest.

In the following, we briefly describe very similar structures but the distinct class of the dictionary sparse signals; *analysis-sparse* and *synthesis-sparse*. The basic concepts of synthesis-sparse and analysis-sparse signals explained in [20], [8], and [21]. Here we only provide a brief review of the main ideas.

- **Synthesis-sparse signals.** We generate this type of signal as follows: first, we choose s columns (atoms) of the dictionary D at random (Note that the index set denotes by T). Second, the value of non-zeros coordinates of x select from a random distribution (e.g. normal distribution). Finally, the s -synthesis signal f create by multiplying D to the sparse coefficient vector x .
- **Analysis-sparse signals.** We use *cosaprsity*¹ to explain the analysis-sparse investigation as a dual of the synthesis-sparse. Consider $\Omega \in \mathbb{R}^{N \times n}$ stand for analysis operator. First, we choose k rows of analysis operator at random (Note that the index set denotes by Λ). Second, we generate a random vector x with Gaussian iid entries and finally, project it onto the orthogonal complement of the subspace generated by Ω_Λ to attain the cosparsity signal ($f = (I - \Omega_\Lambda^* (\Omega_\Lambda \Omega_\Lambda^*)^{-1} \Omega_\Lambda)$). Ω_Λ denotes the rows of Ω that are indexed by Λ .

If we take a closer look at the definitions given above, we see that in the synthesis-sparse case, by removing columns from D which associated with T , the subspace of signal not changed. In contrast, in the analysis-sparse case, the cosparsity index set ($\langle \omega_i, f \rangle = 0, i \in \Lambda$) define the analysis subspace. In general, the subspace of synthesis-sparse and analysis-sparse are different. However, from all subspace of analysis model, one can construct a synthesis subspace. Fig. 3 shows the process of constructing a dictionary sparse signal and taking measurements in the binary forms.

Throughout this paper, we use a tight frame. The rows of Ω formed a frame if there exist constants $0 < a \leq b < \infty$ such that

$$a \|f\|_2^2 \leq \|\Omega f\|_2^2 \leq b \|f\|_2^2$$

¹The cosparsity of a signal f with respect to $\Omega \in \mathbb{R}^{N \times n}$ equal to number of zeros in Ωf

and Ω called a tight frame if $a = b$. Additionally, we consider $a = b = 1$.

III. SYSTEM MODEL

Here, we describe some dedicated phrases to this paper. We also introduce *Hemisphere projection*. We use the Hemisphere Projection to transfer the measurement model from (4) to (5). Then we explain our adaptive system model for binary measurement and present a block diagram of the system model. Afterward, we summarize the methodology of our approach to design and proof algorithms.

- **Effective sparsity.** The Cauchy-Schwarz inequality, relate l_1 -norm to l_2 -norm of signal $x \in \mathbb{R}^N$ as $\|x\|_1 \leq \sqrt{N} \|x\|_2$. We call a coefficient vector $x \in \mathbb{R}^N$ effectively s -sparse if

$$\|x\|_1 \leq \sqrt{s} \|x\|_2$$

To be more clear, consider a set of effectively sparse signals $\mathcal{K} \in S^{n-1} \cap \sqrt{s} B_1^n$. If we change the sparsity level from 1 to N , the l_1 -ball grows from an inscribed polygon (which consist axis only) to circumscribed polygon (which consist all of S^{n-1}). We use the notation Σ_s^N for the set of s -sparse coefficient and $\Sigma_s^{N,eff}$ for effectively s -sparse coefficient in \mathbb{R}^N .

If the signal of interest was selected from a dictionary sparse set, we say that f is effectively s -synthesis sparse if $f = Dx$ for some $x \in \Sigma_s^{N,eff}$ and effectively s -analysis sparse if $D^* f \in \Sigma_s^{N,eff}$.

- **Effective dimension.** The square of the mean width of a set \mathcal{K} , $w^2(\mathcal{K})$, called effective dimension. The effective dimension of the set \mathcal{K} is robust to a small perturbation (a small perturbation in \mathcal{K} change the effective dimension slightly).
- **Pre-image set.** For a (non-invertible) matrix M , We denote $M^{-1}(\mathcal{K})$ for pre-image of set \mathcal{K} with respect to M . In our discussion, the pre-image set D^* , is equal to $\text{Range}(\Omega)$ for analysis-sparse dictionary and the sparse coefficient set ($\text{Span}(x)$) for synthesis-sparse dictionary.

Now, we present the hemisphere projection.

Definition 3 (Hemisphere projection). Let $f \in \mathbb{R}^N$ be an arbitrary signal and $\sigma > 0$ be radius of hemisphere. we

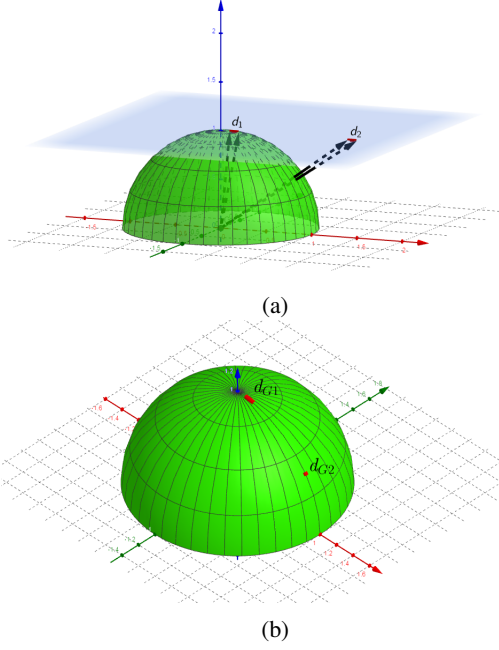


Fig. 4. The geometric interpretation of hemisphere projection.s

define lifted \mathbf{f} as $\tilde{\mathbf{f}} := [\mathbf{f}^T | \sigma]^T \in \mathbb{R}^{N+1}$ and its projection to hemisphere as

$$P_H(\tilde{\mathbf{f}}) = \frac{\tilde{\mathbf{f}}}{\|\tilde{\mathbf{f}}\|_2}. \quad (7)$$

The definition (3) is simple. Nevertheless, geometric interpretation of the hemisphere projection has special benefits in our work. A remarkable point in our work is that the hemisphere projection changes the distance between two vectors. In order to clarify, let us give an example. Let $\mathbf{f}_1 = [0.1, 0]^T$, $\mathbf{f}_2 = [0.2, 0]^T$, $\mathbf{f}_3 = [1, 0]^T$, and $\mathbf{f}_4 = [1.1, 0]^T$ be 4 points on plane $z = 1$. It is obvious the distance between \mathbf{f}_1 and \mathbf{f}_2 is equal to the distance between \mathbf{f}_3 and \mathbf{f}_4 ($d_1 = \|\mathbf{f}_1 - \mathbf{f}_2\|_2 = d_2 = \|\mathbf{f}_3 - \mathbf{f}_4\|_2 = 0.1$). We consider $\sigma = 1$ and put the center of our hemisphere on $[0, 0, 0]^T$ (See Fig.4a). Next, we compute the normalized geodesic distance of the projected points (See Fig.4b). In this example, we have

$$\begin{aligned} d_{G1} &= d_G(P_H(\tilde{\mathbf{f}}_1), P_H(\tilde{\mathbf{f}}_2)) = 0.0311 \\ d_{G2} &= d_G(P_H(\tilde{\mathbf{f}}_3), P_H(\tilde{\mathbf{f}}_4)) = 0.0103. \end{aligned}$$

The difference came from the non-uniformity of hemisphere projection and increased for points with the larger norm. We can control this difference by changing the value of σ . In our application, we use the hemisphere projection intuition to explain our conversion procedure.

Suppose that $\mathbf{f} \in \mathbb{R}^n$ is an effective s -analysis sparse or s -synthesis sparse signal. Let \mathbf{A} be the measurement matrix and $\mathbf{e} \in \mathbb{R}^n$ denote pre-quantization noise with bounded l_∞ -norm. In contrast to the existing method for binary dictionary sparse signal recovery which takes all of the measurements in one step with fixed settings, we solve the problem in a multi-stage. We update thresholding settings through the measurements process. Keep in mind that \mathbf{A} is fixed to avoid the useless

measurements, as far as possible. We define our adaptive threshold as $\varphi^{(i)} \in \mathbb{R}^n$ (see Fig.5).

A. Single-Step Recovery

Throughout our adaptive procedure, we can use the intermediary solution as an estimation of our desired answer. We investigate each iteration of the algorithm individually and call it single-step recovery. In the single-step recovery, we determine the measurement matrix \mathbf{A} and corresponding threshold vector $\boldsymbol{\tau}$. Theorem 2 shows the relation between the number of measurements and reconstruction error for single-step recovery.

Theorem 2 (Single-Step Recovery). *Let $\epsilon, r, \sigma, C, c', \gamma > 0$, and let $\mathbf{A} \in \mathbb{R}^{m \times n}$ be populated by independent standard normal random variables and τ_i for $i = 1, \dots, m$ selected from normal distribution with mean zero and variance σ^2 and independent from \mathbf{A} . Consider $\mathbf{f} \in \mathbb{R}^n$ as an s -analysis (synthesis) sparse vector with $\|\mathbf{f}\|_2 \leq r$. If we take $m \geq C (r/\sigma + \sigma/r)^6 (r^2/\sigma^2 + 1) \epsilon^{-6} s \ln(eN/s)$ measurements using (5), Then, with failure probability at most $\gamma \exp(-c' m \epsilon^2 r^2 \sigma^2 / (r^2 + \sigma^2)^2)$, the solution of*

$$\Delta : \min_{\mathbf{h} \in \mathbb{R}^n} \|\mathbf{D}^* \mathbf{h}\|_1 \quad \text{s.t.} \quad \mathbf{y} = \text{sign}(\mathbf{A} \mathbf{h} - \boldsymbol{\tau}), \|\mathbf{h}\|_2 \leq r, \quad (8)$$

(denote by $\hat{\mathbf{f}}$) satisfies

$$\|\mathbf{f} - \hat{\mathbf{f}}\|_2 \leq \epsilon r. \quad (9)$$

In the next section, we provide our main results which demonstrate:

- How adaptive thresholding algorithm works
- How to compute the number of measurements as a function of effective dimension

IV. MAIN RESULT

Our goal in this paper is to design an adaptive thresholding algorithm based on convex programming to achieve exponential decay in reconstruction error. We have provided a mathematical framework to guarantee our algorithm results.

Theorem 3 (Main theorem). *Consider $\mathbf{A} \in \mathbb{R}^{m \times n}$ as a measurement matrix with standard normal coordinates. Let Δ as single-step recovery scheme, \mathcal{Q} and \mathcal{R} as adaptive quantization and adaptive recovery algorithms respectively and thresholds given by Φ . Fix $r > 0$ and set $\lambda := m/s \log(eN/s)$. With probability at least $1 - C\lambda \exp(-cs \log(eN/s))$, for all $\mathbf{f} \in (\mathbf{D}^*)^{-1} \Sigma_s^{N, \text{eff}}$ in the measurement model:*

$$y_i = \text{sign}(\langle \mathbf{a}_i, \mathbf{x} \rangle - \varphi^{(i)}) \quad (10)$$

the output of \mathcal{R} satisfies

$$\|\mathbf{x} - \hat{\mathbf{x}}\|_2 \leq r 2^{-c\lambda}. \quad (11)$$

Proof. We provide an intuitive proof in IV-D. ■

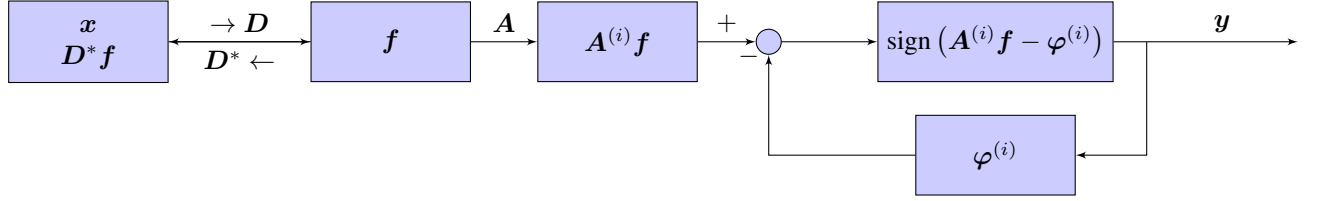


Fig. 5. Block diagram of our adaptive model for dictionary sparse signals

A. High Dimensional Threshold

Our algorithm for high dimensional thresholding given below in Algorithm 1. The algorithm output consists of two parts. The first part is a deterministic point in the signal space which obtained by approximate solution of past stage. This point specifies the center of the set \mathcal{K} _which we want to tessellate it_ and initialized to zero for the first stage. The second part creates random dithers around the center.

Algorithm 1 Φ : High dimension threshold generator

Input: Mapping matrix \mathbf{A} , number of measurements b , dithers variance σ^2 , signal estimation $\hat{\mathbf{f}}$.

Output: High dimension threshold vector $\varphi \in \mathbb{R}^b$.

- 1: $\tau \sim N(0, \sigma^2 \mathbf{I}_b)$
 - 2: $\varphi = \mathbf{A}\hat{\mathbf{f}} + \tau$
 - 3: **return** φ
-

In conventional thresholding algorithms, the only controllable parameter is thresholds variance (σ^2) or equivalently distance from center. In order to clarify the difference of our thresholding scheme, consider the following example in \mathbb{R}^2 .

Let $\mathbf{A} \in \mathbb{R}^{4 \times 2}$ be populated by independent standard normal random variables. Furthermore, consider $\tau_1 \sim N(0, \sigma_1^2 \mathbf{I}_4)$ and $\tau_2 \sim N(0, \sigma_2^2 \mathbf{I}_4)$ as dither vectors with $\sigma_2 < \sigma_1$. Assuming the \mathbf{f} signal as an interesting signal, the geometric interpretation of measurement model (5) has been shown in Fig. 6a. whereas, for the same number of measurements, if we use our measurement model (equation (10)) with early estimates $\hat{\mathbf{f}}$, we are able to reduce the dithers variance and tessellate the smallest set around the desired signal (see Fig. 6b).

In the Algorithm 1, we need measurement matrix \mathbf{A} and signal estimation $\hat{\mathbf{f}}$ to transmit the center of tessellation from zero to $\hat{\mathbf{f}}$ in signal space. we also need dither variance σ^2 to change the hyperplane density around $\hat{\mathbf{f}}$. The Algorithm 1, consist of 3 step. First, generate thresholds dithers. Second, moving thresholds in the amount of $\mathbf{A}\hat{\mathbf{f}}$ and in the last step, the computed threshold is sent to the output.

B. Adaptive Quantization

Our adaptive quantization algorithm is given below in Algorithm 2. To run this algorithm, we need the dictionary \mathbf{D} (which the desired signal is sparse in it), the measurement matrix \mathbf{A} , linear measurement $\mathbf{A}\mathbf{f}$ and an upper norm estimation of signal r ($\|\mathbf{f}\|_2 \leq r$). we initialize first signal estimation to zero. By choosing the number of iterations L and divide the measurement matrix and linear measurement vector to L blocks, we can start the adaptive quantization process.

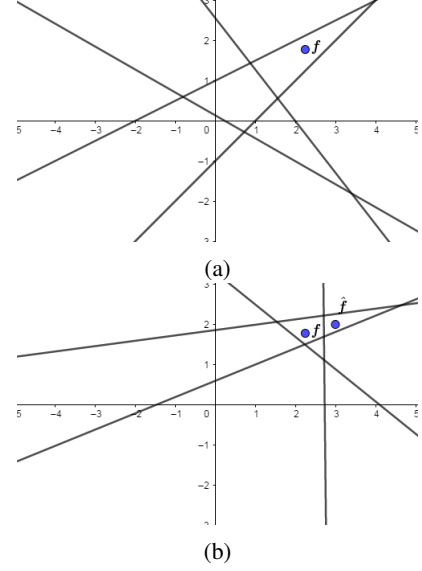


Fig. 6. The geometric interpretation of difference between measurement model (5) and (10)

The adaptive quantization process consists of 3 essential steps. First, in step 2 of pseudo code, we generate the high dimensional thresholds using Algorithm 1. Second, we compare linear measurement block with thresholds and obtain block measurements vector (step 3). Third, compute the estimation of the solution by run single-step recovery (8) with specified parameters. Finally, the Algorithm 2 sends binary measurements vector and threshold values to the output.

Algorithm 2 \mathcal{Q} : Adaptive Quantization

Input: Dictionary $\mathbf{D} \in \mathbb{R}^{n \times N}$, measurement matrix $\mathbf{A} \in \mathbb{R}^{m \times n}$, linear measurement $\mathbf{A}\mathbf{f} \in \mathbb{R}^m$, norm estimation $\|\mathbf{f}\|_2 \leq r$, number of blocks L .

Output: Quantized measurements $\mathbf{y} \in \{\pm 1\}^m$, high dimension thresholds $\varphi \in \mathbb{R}^m$

Initialisation: $\mathbf{f}_0 \leftarrow \mathbf{0}$, $b = \lfloor \frac{m}{L} \rfloor$, $\mathbf{A}^{(i)} \in \mathbb{R}^{b \times m}$

- 1: **for** $i = 1, \dots, L$ **do**
 - 2: $\varphi^{(i)} \leftarrow \Phi(\mathbf{A}^{(i)}, b, 2^{1-i}r, \mathbf{f}_i)$
 - 3: $\mathbf{y}^{(i)} = \text{sign}(\mathbf{A}^{(i)}\mathbf{f} - \varphi^{(i)})$
 - 4: $\mathbf{f}_{i+1} \leftarrow \Delta(\mathbf{D}, \mathbf{A}^{(i)}, \mathbf{y}^{(i)}, \varphi^{(i)}, r)$
 - 5: **end for**
 - 6: **return** $\mathbf{y}^{(i)}, \varphi^{(i)}$ for $i = 1, \dots, L$
-

C. Adaptive Recovery

In the Recovery procedure (Algorithm 3), we need the dictionary \mathbf{D} , the measurement matrix \mathbf{A} , binary measurements vector \mathbf{y} , high dimension threshold vector $\boldsymbol{\varphi}$ and an upper norm estimation of signal r . In the adaptive recovery algorithm, we first divide the inputs to the L blocks. Then, we simply run the single-step recovery on each block.

A notable point in the adaptive recovery is the duplication of operation. If we take a closer look at the adaptive quantization, we will see that Algorithm 3 is a part of Algorithm 2. We can use the adaptive recovery algorithms when linear measurements are not available and we have access to the binary measurements vector.

Algorithm 3 \mathcal{R} : Adaptive Recovery

Input: Dictionary $\mathbf{D} \in \mathbb{R}^{n \times N}$, measurement matrix $\mathbf{A} \in \mathbb{R}^{m \times n}$, quantized measurements $\mathbf{y} \in \{\pm 1\}^m$, high dimension thresholds $\boldsymbol{\varphi} \in \mathbb{R}^m$, norm estimation $\|\mathbf{f}\|_2 \leq r$, number of blocks L .

Output: Estimated vector $\hat{\mathbf{f}} \in \mathbb{R}^n$.

Initialisation: $b = \lfloor \frac{m}{L} \rfloor$, $\mathbf{A}^{(i)} \in \mathbb{R}^{b \times m}$, $\mathbf{y}^{(i)} \in \{\pm 1\}^b$, $\boldsymbol{\varphi}^{(i)} \in \mathbb{R}^b$

- 1: **for** $i = 1, \dots, L$ **do**
 - 2: $\mathbf{f}_i \leftarrow \Delta(\mathbf{D}, \mathbf{A}^{(i)}, \mathbf{y}^{(i)}, \boldsymbol{\varphi}^{(i)}, r)$
 - 3: **end for**
 - 4: **return** \mathbf{f}_L
-

D. Intuitive proof of main theorem

Here, we provide an intuitive proof of Theorem 3. Let's start with reviewing the expression. Briefly, in this theorem, we run the single-step recovery for different dithers and center in L stage. We use results from conventional one-bit compressed sensing to prove this theorem. The hemisphere projection acts as a bridge between the conventional one-bit compressed sensing and our work.

Consider a hemisphere with radius σ and center the origin. This Hemisphere touch signal space of \mathbf{f} at $[\mathbf{0}^T | \sigma]^T \in \mathbb{R}^{n+1}$. Remember that each row of the matrix \mathbf{A} specifies a hyperplane in \mathbb{R}^n . This hyperplane can be considered as another hyperplane in \mathbb{R}^{n+1} which passes through the origin. Nevertheless, the new signal space _after projection_ is the upper half of σS^n . Now we can use random hyperplane tessellation to limit the error. As mentioned above we initialized the algorithm with an upper estimation of $\|\mathbf{f}\|_2$ and this leads to creating large cells on the hemisphere's shell. In each step, the algorithm 1 moves the hemisphere to the estimated pint and the size of the hemisphere reduced as regards reduction of σ . This reduction improves the resolution of mapping and leads to error decrement.

V. NUMERICAL EXPERIMENTS

In this section, we explore the performance our algorithm and compare it to the performance of previous one-bit dictionary sparse recovery given by [9]. The computations, per-

formed in MATLAB using the CVX package, are reproducible and can be downloaded from Here².

The experimental setup is as follows. The coordinate of random measurements matrix $(a_{i,j})$ were generated as a standard normal distribution. The s -sparse coordinate of $\mathbf{x} \in \mathbb{R}^N$ for $N = 1000$ selected from uniform random distribution and the values of magnitude are chosen from standard normal distribution. we use redundant dictionary $\mathbf{D} \in \mathbb{R}^{n \times N}$ ($N = 1000, n = 50$) which forms as follow. First, we construct a matrix where it is columns are drawn randomly and independently from S^{n-1} . Then, we define our thigh dictionary as an orthonormal basis of the column space of this matrix.

We compare our algorithms result with two convex programming based algorithms, demonstrated in [9]. The first algorithm solves linear programming optimization (LP) [9, Subsection 4.1] and the second algorithm solves second-order cone programming (CP) optimization [9, Subsection 4.2]. These algorithms use the measurement model (5). We generate the threshold coordinates (τ_i) from an independent normal distribution with mean zero and variance σ^2 . In our algorithm, we set the overestimate of the norm of \mathbf{f} to $r = 2 * \|\mathbf{f}\|_2$. We also set $\sigma = r$ for LP and CP algorithms. We define the normalized reconstruction error as $\|\mathbf{f} - \hat{\mathbf{f}}\|_2 / \|\mathbf{f}\|_2$. In the our algorithm we set number of blocks $L = 10$.

For each sample of figures we run the simulation 50 times and plot the average of results.

Fig. 7 shows the experiment result for sparsity level 10. As it is clear from the Fig. 7 LP algorithm behaviors similar to CP (LP algorithm outperforms CP by 2dB on average). Our algorithm, in fewer samples, behaves slightly weaker than others. But, it seems to be a phase transition when the number of measurements increased and as we see in Fig. 7 our proposed algorithm substantially works better than LP and CP (Over **50dB** in steady-state condition!).

In the second experiment, we examine the performance of our algorithm for multiple degrees of sparsity. Fig. 8 shows the result for $s = 10, 20, 30, 40, 50$ (we assumed other parameters as the first experiment). As it is clear from the figure, by increasing the sparsity level, our accuracy decreased.

VI. CONCLUSIONS AND FUTURE WORK

In this paper, we proposed an algorithm which exploits the inherent information in the sampling procedure adaptively. This scheme helps to substantially reduce the number of needed measurements. In addition, our algorithm exhibits an exponential decaying behavior in reconstruction error. The proof approach is based on geometric theories in the high dimensional estimation. In this work, we used geometric intuition to explain our result which can be used in other areas of signal processing. We believe our analysis can be extended to the multi-bit setting. Throughout this work, we used a fixed reduction pattern in the thresholds dithers. We believe this reduction can be smart by extracting the geometric features in each step of the algorithm.

²<https://gitlab.com/HosseinBeheshti/AdaptiveBDS>

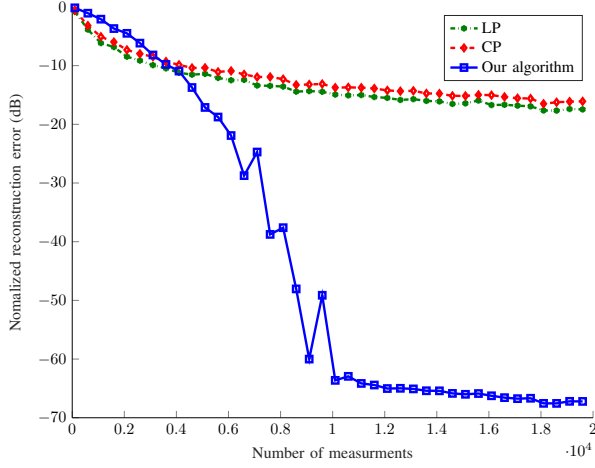


Fig. 7. Averaged reconstruction error by the outputs of Algorithms LP, CP, and algorithm 2

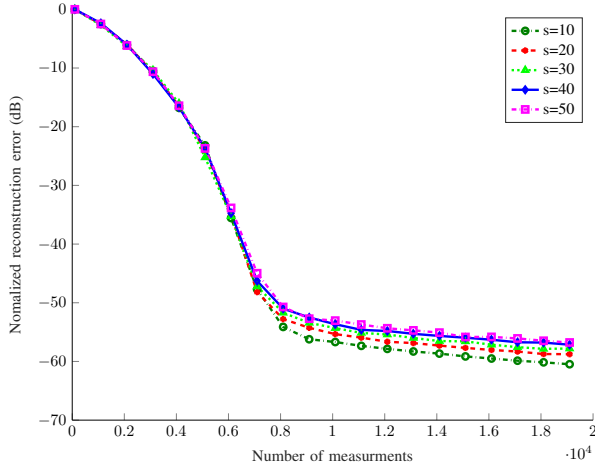


Fig. 8. Algorithm behavior for $s = 10, 20, 30, 40, 50$

REFERENCES

- [1] D. L. Donoho, "Compressed sensing," *IEEE Transactions on information theory*, vol. 52, no. 4, pp. 1289–1306, 2006.
- [2] E. J. Candès *et al.*, "Compressive sampling," in *Proceedings of the international congress of mathematicians*, vol. 3, pp. 1433–1452, Madrid, Spain, 2006.
- [3] P. T. Boufounos and R. G. Baraniuk, "1-bit compressive sensing," in *Information Sciences and Systems, 2008. CISS 2008. 42nd Annual Conference on*, pp. 16–21, IEEE, 2008.
- [4] H. Yin, Z. Wang, L. Ke, and J. Wang, "Monobit digital receivers: design, performance, and application to impulse radio," *IEEE Transactions on Communications*, vol. 58, pp. 1695–1704, jun 2010.
- [5] C. Risi, D. Persson, and E. G. Larsson, "Massive mimo with 1-bit adc," *arXiv preprint arXiv:1404.7736*, 2014.
- [6] L. Jacques, J. N. Laska, P. T. Boufounos, and R. G. Baraniuk, "Robust 1-bit compressive sensing via binary stable embeddings of sparse vectors," *IEEE Transactions on Information Theory*, vol. 59, no. 4, pp. 2082–2102, 2013.
- [7] R. G. Baraniuk, S. Foucart, D. Needell, Y. Plan, and M. Wootters, "Exponential decay of reconstruction error from binary measurements of sparse signals," *IEEE Transactions on Information Theory*, vol. 63, no. 6, pp. 3368–3385, 2017.
- [8] E. J. Candès, Y. C. Eldar, D. Needell, and P. Randall, "Compressed sensing with coherent and redundant dictionaries," *Applied and Computational Harmonic Analysis*, vol. 31, pp. 59–73, jul 2011.
- [9] R. Baraniuk, S. Foucart, D. Needell, Y. Plan, and M. Wootters, "One-bit compressive sensing of dictionary-sparse signals," *Information and Inference: A Journal of the IMA*, vol. 7, pp. 83–104, aug 2017.
- [10] J. N. Laska and R. G. Baraniuk, "Regime change: Bit-depth versus measurement-rate in compressive sensing," *IEEE Transactions on Signal Processing*, vol. 60, no. 7, pp. 3496–3505, 2012.
- [11] P. T. Boufounos, "Greedy sparse signal reconstruction from sign measurements," in *2009 Conference Record of the Forty-Third Asilomar Conference on Signals, Systems and Computers*, pp. 1305–1309, IEEE, 2009.
- [12] J. N. Laska, Z. Wen, W. Yin, and R. G. Baraniuk, "Trust, but verify: Fast and accurate signal recovery from 1-bit compressive measurements," *IEEE Transactions on Signal Processing*, vol. 59, no. 11, pp. 5289–5301, 2011.
- [13] Y. Plan and R. Vershynin, "One-bit compressed sensing by linear programming," *Communications on Pure and Applied Mathematics*, vol. 66, no. 8, pp. 1275–1297, 2013.
- [14] Y. Plan and R. Vershynin, "Robust 1-bit compressed sensing and sparse logistic regression: A convex programming approach," *IEEE Transactions on Information Theory*, vol. 59, no. 1, pp. 482–494, 2013.
- [15] K. Knudson, R. Saab, and R. Ward, "One-bit compressive sensing with norm estimation," *IEEE Transactions on Information Theory*, vol. 62, no. 5, pp. 2748–2758, 2016.
- [16] U. S. Kamilov, A. Bourquard, A. Amini, and M. Unser, "One-bit measurements with adaptive thresholds," *IEEE Signal Processing Letters*, vol. 19, no. 10, pp. 607–610, 2012.
- [17] C. S. Gntrk, "One-bit sigma-delta quantization with exponential accuracy," *Communications on Pure and Applied Mathematics*, vol. 56, pp. 1608–1630, jul 2003.
- [18] R. Vershynin, "Estimation in high dimensions: a geometric perspective," in *Sampling theory, a renaissance*, pp. 3–66, Springer, 2015.
- [19] Y. Plan and R. Vershynin, "Dimension reduction by random hyperplane tessellations," *Discrete & Computational Geometry*, vol. 51, no. 2, pp. 438–461, 2014.
- [20] M. Elad, P. Milanfar, and R. Rubinstein, "Analysis versus synthesis in signal priors," *Inverse problems*, vol. 23, no. 3, p. 947, 2007.
- [21] S. Nam, M. E. Davies, M. Elad, and R. Gribonval, "The cospase analysis model and algorithms," *Applied and Computational Harmonic Analysis*, vol. 34, no. 1, pp. 30–56, 2013.